We are IntechOpen, the world's leading publisher of Open Access books
Built by scientists, for scientists

6,900
Open access books available

186,000
International authors and editors

200M
Downloads

Our authors are among the

154
Countries delivered to

TOP 1%
most cited scientists

12.2%
Contributors from top 500 universities

CLARIVATE ANALYTICS
BOOK CITATION INDEX
INDEXED

WEB OF SCIENCE™

Selection of our books indexed in the Book Citation Index
in Web of Science™ Core Collection (BKCI)

Interested in publishing with us?
Contact book.department@intechopen.com

Numbers displayed above are based on latest data collected.
For more information visit www.intechopen.com

Metal-Oxide Nanowires for Gas Sensors

Supab Choopun, Niyom Hongsith and
Ekasiddh Wongrat

Additional information is available at the end of the chapter

http://dx.doi.org/10.5772/54385

1. Introduction

In past decades, gas sensors based on the metal oxide semiconductors (MOSs) have been studied in diverse field for wide applications. A gas sensor is a device that can be used to detect various gas such as ethanol, LPG, CO_2 and CO gases etc. The gas sensors based on MOSs such as SnO_2, TiO_2, WO_3, ZnO, Fe_2O_3, and In_2O_3 have an important role in environmental monitoring, chemical process controlling, personal safety (Q. Wan et al., 2004), industrial process controls, for the detection of toxic environmental pollutants in human health, and for the prevention of hazardous gas leaks, which comes from the manufacturing processes (K. Arshak&I. Gaidan, 2005), wine quality monitoring, and traffic safety (X.F. Song et al., 2009).

The first generation of MOS gas sensors were based on thick films of SnO_2 since 1960s which was firstly reported by Taguchi (E. Comini et al., 2009). The MOS gas sensors have some advantages such as small size, low-power-consumption (E. Comoni et al., 2009), simple construction, good sensing properties (K. Arshak&I. Gaidan, 2005), and high compatibility with microelectronic processing (E. Comini et al., 2002). So, they have rapidly gained attention over the years.

Recently, various morphologies of MOS nanostrcutures such as wire-like, belt-like, rod-like, and tetrapods have been widely investigated for gas sensor applications. It is well-known that the sensitivity characteristics of these sensors strongly depend on the morphology of MOS. Especially, one-dimensional nanostructures such as nanowires, nanobelts, nanoneedles have gained a lot of interest for nanodevice design and fabrication (Wang et al., 2008). The sensors based on MOS nanowires are promising due to feasibility for ultrahigh sensitive sensors or ppb-level sensors. These nanowires can be prepared by various techniques such as pulse laser deposition (PLD), chemical vapor deposition (CVD), thermal evaporation, metal-catalyzed

molecular beam epitaxy (CBE) and thermal oxidation technique. Moreover, there are many reports on gas sensor based on the nanowires.

The fundamental mechanism of gas sensing based on MOS depend on the reaction between the surface complexes such as O^-, O^{2-}, H^+, and OH^- reactive chemical species and the gas molecules (reducing/oxidizing gas) to be detected (E. Comini et al., 2009). Thus, it is important to understand the surface reactions between semiconductor surface and target gas for improving the sensing characteristics. Typically, the important parameters in sensor development are sensitivity, selectivity, and stability that called "3S" (E. Comini et al., 2009). However, in this chapter we will mostly discuss on only the sensitivity parameter.

The sensitivity of sensors based on bulk and thin film MOS is typically low. Thus, sensitivity improvement has been extensively studied by using several techniques. The two techniques that commonly used for sensitivity improvement are in the following:

1. *Using nanostructures*

The MOS sensors based on various nanostructures such as nanowires, nanobelts, nanoparticles, nanrods, and nanotubes etc. have been demonstrated to be excellent candidates for ultrahigh sensitivity due to their high surface-to-volume ratio. A large surface-to-volume ratio means that a significant fraction of atoms (or molecules) are much quantity on the surface. So, the reaction between target gas and reactive chemical species (O^-, O^{2-}, H^+, and OH^-) on the surface can extremely occur. A list of MOS sensors with the sensitivity for the different morphologies of ZnO nanostructures is summarized in Table 1. It can be seen that the sensor sensitivity strongly depends on size and morphology of ZnO nanostructures.

2. *Adding noble metal*

The noble metals such as Au, Pt, Pd, and Ag on the surface of MOSs can act as a catalyst to modify surface reactions of MOSs toward sensing gas and result in high sensitivity. The ZnO sensors with noble metal additive are also listed in Table 1.

Usually, the gas sensors based on MOS nanostructures exhibit high sensitivity and sometimes up to a few hundred folds over a conventional MOS sensor at a moderate concentration. On the other hand, the sensors based on a larger size of MOS such as in the form of thin film or micro-tetrapod shows lower sensitivity. Several models have been proposed to explain sensitivity characteristics of MOS sensors and still be a subject of discussion.

There are many reports about gas sensor model that are used to explain sensor response characteristics. Wang and co-workers have proposed a surface-depletion model and a contact-controlled model that are used to describe the sensing mechanism of resistance-type metal-oxide semiconductor sensors (Feng et al., 2005). The surface-depletion controlled model is used to explain the sensing mechanism of semiconducting oxide sensors based on nanocrystal/nanowire/nanobelt structures, while the contact-controlled model is proposed to explain the contact between the outer ends of the rods. This leads to the formation of many junctions in the sensors that significantly modify the potential barrier of contact between rods. These barriers can control the transport of electrons between the rods resulting in the change of the sensor resistance. Chen and co-workers (Chen et al., 2006) have used space-charge model to

explain the sensitivity improvement when the grain size is close to or smaller than the Debye length ($2L_d$).

In this chapter, we investigate the sensing characteristics of the MOS nanowire sensors and present the sensitivity formulas that are developed in order to explain all circumstances of gas sensors based on MOS nanowires. The size and morphology dependences on the sensitivity are explained in terms of the two important parameters including surface-to-volume ratio and depletion layer width. The developed formulas will be discussed and related to the experimental sensing characteristics of ZnO sensors.

Materials	Morphology	Diameter (nm)	Target gas	Sensitivity (ppm)										
				1	10	25	50	100	150	200	300	500	1000	2000
ZnO (Son et al., 2008)	nanowire	20	Ethanol	~16		~40	~54	~62	~70	~70		-	-	
ZnO (Xu et al., 2008)	nanorod	40-80	Ethanol				7.3	-				-	-	
ZnO (Chen et al., 2006)	nanorod	<15	Ethanol		20.5		104.9	176.8		224.2		267.7	-	
ZnO (Bie et al., 2007)	nanorod	10-30	Ethanol		~5		~10	18.29				~32	~42	
ZnO (Li et al., 2009)	nanoneedle	5-10	Ethanol	11	56		116	176		~300		~650	-	
ZnO (Wan et al., 2004)	nanowire	25	Ethanol	~2.5		~8	~16	~33		~47		-	-	
ZnO (Feng et al., 2005)	flowerlike	150	Ethanol	2.2	5.8		11.4	14.6				25.2	30.1	
ZnO (Li et al., 2007)	nanorod	15	Ethanol	4.1	10.7		18.1	29.7				~72	100	
ZnO (Yang et al., 2008)	nanorod	50	Ethanol	10	18		60	100				-	-	
ZnO (Chen et al., 2008)	nanotube	250	Ethanol	2.6			-	24.1		34.8		59.3	-	
ZnO (Choopun et al., 2007)	nanobelt	50-150	Ethanol				7.3		12			21.1	23.2	
ZnO (Hongsith et al., 2008)	nanowire	60-180	Ethanol				-	5.07				9.79	14	14
ZnO (Wongrat et al., 2009)	nanowire	100-500	Ethanol				2	3				5	8	
SnO$_2$ (Neri et al., 2006)	nanopowder	6-100	Ethanol				~7	~8.6	~10			-	-	
SnO$_2$ (Lee et al., 2008)	nanorod	<100	Ethanol				-	-				-	~40	
ZnO (Liu et al., 2010)	nanotube	200	H$_2$				-	2.3				-	-	
ZnO (Bie et al., 2007)	nanorod	10-30	H$_2$		~5		~7	10.41				~22	~24	
SnO$_2$ (Zhang et al., 2010)	nanofiber	80-120	H$_2$				~2	~5				~8	~10	
SnO$_2$ (Lee et al., 2008)	nanorod	<100	H$_2$				-	-				-	~10	
SnO$_2$-Pd (Zhang et al., 2010)	nanofiber	80-120	H$_2$				~5	~8				~15	~26	

Materials	Morphology	Diameter (nm)	Target gas	Sensitivity (ppm)										
				1	10	25	50	100	150	200	300	500	1000	2000
SnO$_2$-Pd (Lee et al., 2008)	nanorod	<100	H$_2$				~33	-				-	~700	
ZnO-Au (Hongsith et al., 2008)	nanowire	60-180	Ethanol				-	6				12	24	37
SnO$_2$-Pt (Neri et al., 2006)	nanopowder	6-100	Ethanol				~18	26.5	~31			-	-	
SnO$_2$-Pd (Lee et al., 2008)	nanorod	<100	Ethanol				~15	-				-	~125	
ZnO-Au (Li et al., 2007)	nanorod	15	Ethanol			20.1	41.8	89.5			193.6	-	-	
ZnO-Au (Wongrat et al., 2009)	nanowire	100-500	Ethanol				7	10				20	32	

Table 1. List of MOS sensors with the sensitivity for the different morphologies of ZnO nanostructures.

2. Sensing mechanism and sensitivity parameters

Normally, the gas sensor based on MOS has an optimum operating temperature at high temperature about 250-350°C. When the MOS is heated at lower temperature about 100-200°C, oxygen molecules in the atmosphere are adsorbed on its surface and form oxygen ion molecules by attracting an electron from the conduction band of MOS as shown in the Eq. (1).

$$O_2(gas) + e^- \Leftrightarrow O_2^-(adsorb) \tag{1}$$

At higher temperature, the oxygen ion molecules are dissociated into oxygen ion atoms with singly or doubly negative electric charges by attracting an electron again from the conduction band as shown in Eq. (2) and (3)

$$\frac{1}{2}O_2 + e^- \overset{k_{Oxy}}{\Leftrightarrow} O_{ads}^- \tag{2}$$

$$\frac{1}{2}O_2 + 2e^- \overset{k_{Oxy}}{\Leftrightarrow} O_{ads}^{2-} \tag{3}$$

where k_{Oxy} is the reaction rate constant. The oxygen ions on the surface of MOS are extremely active with the target gas molecule and give up the electrons from the surface back to the conduction band of MOS. The generally chemical reaction between gas molecule and oxygen ions is shown in Eq. (4)

$$X + O_{ads}^{b-} \xrightarrow{k_{gas}} X' + be^-$$ (4)

where X and X' is target gas and out gas, respectively. The b value is the number of electron and k_{gas} is the reaction rate constant of the gas reaction.

The chemical reaction causes change of the carrier concentration in the conductivity and thus, change of sensor resistance. The change of sensor resistance depends on a type of MOSs. A schematic diagram for change of the sensor resistance upon exposure to the target gas (reducing gas) in the cases of n-type and p-type MOS sensors is illustrated in Fig 1 and will be discussed in the following.

2.1. -type metal oxide gas sensor

Since majority carriers in n-type MOSs are electron, the resistance of n-type MOS sensor decreases when the temperature increases due to their semiconducting properties. However under oxygen ambient, from Eq. (1)-(3), the electrons in the conduction band of n-type MOS are removed by the adsorbed oxygen ions. This causes a decrease of the carrier concentration and thus, an increase of resistance of n-type MOS sensor at operating temperature. When the n-type MOS sensor is under the target gas ambient (reducing gas), the electrons obtained from the chemical reaction as in Eq. (5) are given back to the conduction band leading to a decrease of the sensor resistance.

2.2. p-type metal oxide gas sensor

In another hand, the majority carriers in p-type MOSs are holes. Similar to n-type MOSs, the sensor resistance of p-type MOS decreases when the temperature increases. However, under oxygen ambient, p-type MOS generates holes when the oxygen ions are adsorbed on the surface via the excited electrons from valence band. This process results in raising the number of charge carriers, which leads to a decrease of the sensor resistance (opposite to n-type). When the p-type MOS sensor is under the target gas ambient (reducing gas), the electrons inject into the valence band and recombine with the holes and this method resulting in reducing the number of holes, which leads to an increase of the sensor resistance (opposite to n-type).

It should be noted that in the case of an oxidizing gas the change of resistance will be just opposite to the above discussions.

In addition, from Eq. (4), a rate equation of an electron density can be written as

$$\frac{dn}{dt} = k_{gas}[O_{ads}]^b[X]^b$$ (5)

where n is the electron density or the electron concentration under the gas atmosphere, and k_{gas} is the reaction rate constant or reaction rate coefficient described as
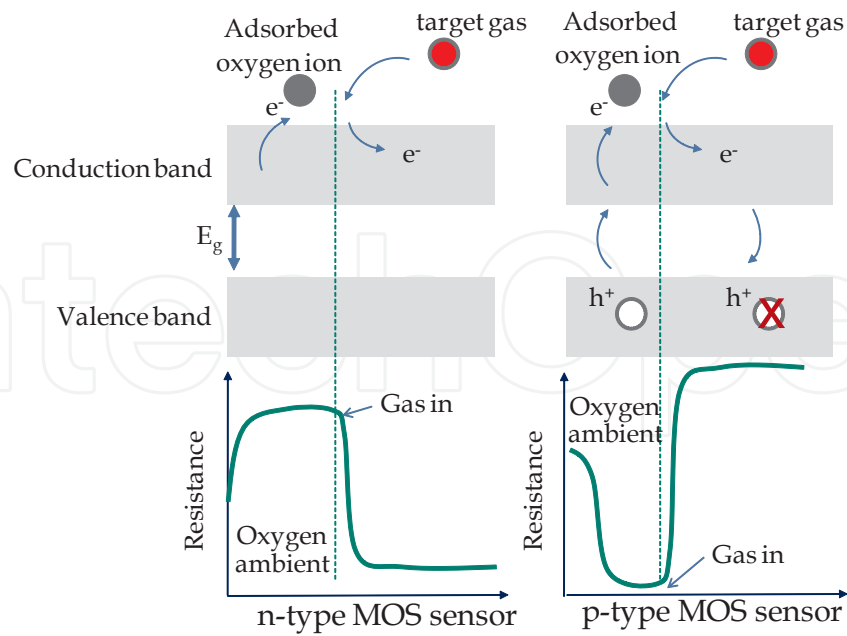
Figure 1. Schematic diagram for change of the sensor resistance upon exposure to the target gas (reducing gas) in the cases of n-type and p-type MOS sensors.

$$k_{gas} = A \exp\left(-E_a / k_B T\right) \tag{6}$$

where E_a is the activation energy of a reaction, k_B is the Boltzmann constant and T is absolute temperature. By integrating Eq. (5) at an equilibrium state under gas ambient and air ambient and using the carrier concentration defined as $n=\alpha/R$ (where R is a resistance and α is a proportional constant), a sensitivity relation can be obtained as (Hongsith et. al, 2010)

$$n = \Gamma_t k_{gas} [O_{ads}^{ion}]^b [X]^b + n_0 \tag{7}$$

$$S_g = \frac{R_a}{R_g} = \frac{\Gamma_t k_{gas} [O_{ads}^{ion}]^b [X]^b}{n_0} + 1 \tag{8}$$

Sometimes, a compact form of the sensitivity relation on gas concentration, X, can be rewritten as

$$S_g = aX^b + 1 \tag{9}$$

where a is a controllable parameter.

Figure 2. a) sensors based on thin film structrue and (b) based on thin films with perpendicular spike nanowires. The sensitivity enhancement of nanowire sensors can be explained by Eq. (11) which is due to an increase of surface-to-volume ratio.

The sensitivity formula in Eq. (8) can be applied to explain very well in the case of thin film and bulk. In the case of nanostructure, however, two important parameters including surface-to-volume ratio and depletion layer width need to consider in order to explain the sensing characteristics.

2.2.1. Surface-to-volume ratio

Generally, this surface-to-volume ratio can be related to the density of the adsorbed oxygen ions. Thus, we have proposed that the density of adsorbed oxygen ions can be written in term of surface-to-volume ratio as

$$[O^{ion}_{ads}] = \frac{\sigma_0 \Phi V_m}{V_s} \qquad (10)$$

where σ_0 is a number of oxygen ions per unit area, Φ is a ratio of surface area per volume of material V_m, and V_s is a system volume. By substituting Eq. (10) onto Eq. (8) gives

$$S_g = \frac{\Gamma_t k_{gas} \left(\dfrac{\sigma_0 \Phi V_m}{V_s} \right)^b}{n_0} X^b + 1 \qquad (11)$$

The Eq. (11) can be applied to explain very well in the case of sensors based on MOS nanowires. At the begining, it is quite amazed that sensors based on MOS nanowires exhibited the sensitivity higher than that of thin film or bulk even though the nanowires were not aligned along the conductive direction. For example, sensors based on thin films with perpendicular spike nanowires as shown in Fig.2 exhibit the sensitivity of higher than sensor based on thin film structure. The explanation of sensitivity enhancement is clear with using the Eq. (11) which is due to an increase of surface-to-volume ratio.
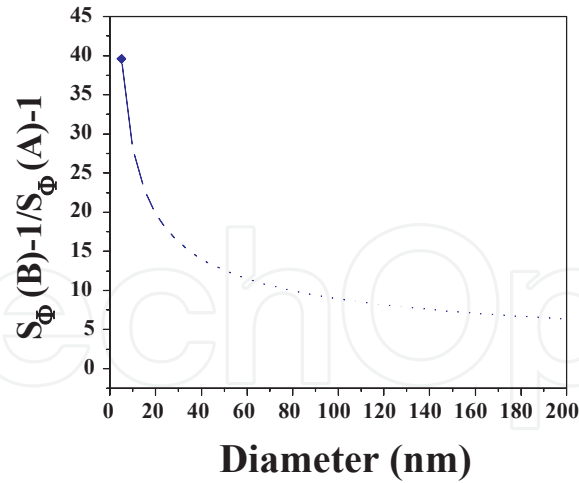
Figure 3. The sensitivity ratio as a function of diameter where L = 10 μm of a gas sensor based on vertical alignment ZnO nanorods with diamerter D and length L and a gas sensor based on ZnO thin films with an area of 1 cm².

From Eq. (11), the sensitivity strongly depends on the surface-to-volume ratio (Φ) as discussed earlier. For example, let consider a thin film with an area of 1 cm² as shown in Fig. 2 (a). Then, given cylindrical nanostructures of 10 μm in length with various diameters are grown on this area, as shown in Fig. 2 (b). The surface-to-volume ratio can be calculated and put in Eq. (11) for the sensitivity ratio as

$$\frac{S_\Phi(B)-1}{S_\Phi(A)-1} = \left(\frac{\Phi_B}{\Phi_A}\right)^b \tag{12}$$

The sensitivity ratio as a function of diameter is plotted as shown in Fig. 3. It can be seen that the sensor sensitivity enhances as decreasing the diameter due to an increase of surface-to-volume ratio and rapidly enhances at small diameter.

2.2.2. Depletion layer width

Typically, the sensor resistance is contributed from two parts including the resistance along a cylindrical nanowire, and the resistance between nanowires. The resistance along the nanowire is due to surface depletion layer and conductive channel. The resistance between nanowires is due to band bending (potential barrier between wires) which depend on a size of nano-structure.

First, let consider for only the resistance along the nanowire by neglecting the resistance between nanowires. According to the depletion layer or the space charge model, L_d (Debye length), can be expressed by

$$L_d = \left(\frac{\varepsilon k_B T}{q^2 n} \right)^{1/2} \tag{13}$$

where ε is a static dielectric constant, q is an electrical charge of a carrier, and n is a carrier concentration. It can be seen that at steady operating temperature, the Debye length depends only on the carrier concentration. Let consider in Eq. (13), at the optimum operating temperature based on pure or undoped MOS nanowire sensor, the L_d can be regarded as a constant value and equals to a value of the depletion layer width.

In this model, a cylinder, which is one of the most basic geometric shapes in one-dimension, is considered and a conductive channel is assumed to be along the axis of the cylinder. At an operating temperature, the oxygen ions are adsorbed by attaching an electron on the surface of the cylinder. Therefore, the depletion layer is formed on the surface of cylinder with a thickness of L_d, and then a size of conductive channel is reduced along the radial direction as shown in Fig. 4.

When exposed to the reducing gas atmosphere, gas reacts with oxygen ions on the surface and gives back electrons to MOS sensors resulting in increasing conductive channel (decreasing depletion layer width). The conductive channel can be related to the carrier concentration, and can be written in term of the depletion layer width (L_d) as

$$n^{/} = n_0 \frac{\pi \left(D - 2L_d \right)^2}{\pi D^2} \tag{14}$$

where n_0 is a carrier concentration of a intrinsic material, n' represents a carrier concentration of the Debye length, and D is a diameter of the cylinder. Thus, the effect of the depletion layer on sensitivity based on cylindrical MOS nanowire are given by inserting Eq. (14) in Eq. (11) and obtained

$$S_{L_d} = \left(\frac{\Gamma_t k_{gas} (\sigma_0 \Phi (V_m / V_s))^b}{n_0} \right) \frac{D^2 X^b}{\left(D - 2L_d \right)^2} + 1 \tag{15}$$

Let compare a diameter of cylinder D to the Debye length (L_d). Since the Debye length is in the order of nanometer, it can be divided into three conditions.

Under condition D >> 2L$_d$, Eq. (15) turns in to Eq. (11)

In this condition, a diameter of cylinder is much larger than micrometer which is the case of microstructure or bulk materials. The depletion layer width is very small compared with the cylindrical diameter ($D >> 2L_d$) and Eq. (15) can be approximated to Eq. (11) which is an equation that has no depletion layer effect.

$D > 2L_d$, Eq. (15) can be approximated to Eq. (11)

When a diameter of cylinder is in the order of nanometer but still larger than Debye length ($D > L_d$), Eq. (15) again can be approximated to Eq. (11) with no depletion layer effect. However, the sensor sensitivity strongly depends on the oxygen ion density due to the surface-to-volume ratio, Φ, parameter.

$D \sim 2L_d$, sensor sensitivity strongly depends on D

When a cylindrical diameter decreases down to the order of nanometer and is comparable to the Debye length ($D \sim 2L_d$), the depletion layer has strong effect and the sensor sensitivity is strongly dependent on a cylindrical diameter. Thus, Eq. (15) can be used to explain sensitivity of all structural size ranging from nanometer to bulk and can be regarded as a general form of sensitivity formula in order to explain the sensing characteristics.

Figure 4. Schematic diagram of the depletion layer on the surface of cylinder with a thickness (or width) of L_d, under condition of $D \gg 2L_d$, $D \gg 2L_d$, and $D \sim 2L_d$ (not in scale).

Second, let consider for a case that sensor resistance is contributed from both along nanowire and between nanowires. So, the sensor resistance is due to both effects of surface deletion layer and band bending (potential barrier). It should be noted that band bending has also effect on the surface depletion layer. Since the sensor resistance strongly depend on a size of nanowire, let compare a diameter of a cylindrical nanowire D with a depletion layer width (w). It can be divided into three cases.

Under $D \gg 2w$ (large size)

In this case, the depletion layer width is much narrow compared to a diameter of the cylinder so the depletion layer has small effect on the electron density in the wires. However, it does greatly affect the potential barrier of the contacts between the wires. Thus, the sensor resistance is dominantly controlled by the potential barrier in this case.

From the oxygen adsorption reaction as given in Eq. (1)-(3) which oxygen ion specie is O^{2-}, at equilibrium condition it can be deduced by using the mass action law that

$$k_a \left[e \right]^2 P^{1/2} = k_d \sigma. \tag{16}$$

$$\sigma = k_{Oxy}\left[e\right]^2 P^{1/2} \tag{17}$$

where k_{Oxy} is an equilibrium constant of oxygen adsorption reaction which is defined as $k_{Oxy} = k_a/k_d$, where k_a and k_d is a reaction constant for oxygen adsorption and desorption

reactions, respectively. σ is a density of O^{2-} per unit area, $[e]$ is a density of conduction electron at the surface, and P is a partial pressure of oxygen molecule. The density of conduction electrons at surface [e] can be expressed in terms of a surface potential as (Yamazoe & Shimanoe, 2008)

$$\left[e\right] = n_0 \exp\left(-\frac{qV_B}{k_B T}\right) \tag{18}$$

where n_0 is a density of donor electron, which is assumed to be constant throughout MOS and the relation between V_B and w is shown as (Yamazoe & Shimanoe, 2008):

$$w = \left(\frac{2\varepsilon}{qn_d}V_B\right)^{1/2} = L_d\left(2\beta V_B\right)^{1/2}, \quad V_B = \frac{\left(w/L_d\right)^2}{2\beta}. \tag{19}$$

Here L_d is the Debye length defined by $L_D = (\varepsilon kT/q^2 N_d)^{1/2}$, and $\beta = q/kT$, where k and T are Boltzmann constant and temperature, respectively. In addition, n_0 is the density of conduction electrons and apparently is equal to the density of donors, n_d. By using Eq. (18), we can rewrite it as (Yamazoe & Shimanoe, 2008):

$$\left[e\right] = n_d \exp\left(-\frac{qV_B}{k_B T}\right). \tag{20}$$

Since the sensor resistance is dominantly controlled by the potential barrier in this case, the sensor resistance R, which is inversely proportional to the electron density is given as (Yamazoe & Shimanoe, 2008)

$$R = R_0 \exp(m^2/2), \quad R \propto \frac{1}{\left[e\right]} \tag{21}$$

where R_0 is a resistance under the flat band condition, m is the reduced depletion depth which is defined by $m = w/L_d$. Moreover, if there are no electron-trapping sites other than the adsorbed oxygen ion O^{2-} on the surface, the depletion layer width (w) can be related to density of O^{2-} per unit area (σ) as (Yamazoe & Shimanoe, 2008):

$$\sigma = n_d w \tag{22}$$

From Eq. (22), the larger depletion layer width results in higher density of O^{2-} per unit area (σ). Finally, the density of O^{2-} per unit area (σ) and $[e]$($[e]=n_0$ in this case) can be inserted into Eq. (15) and give (Wongrat et al., 2012)

$$S_g = \left(\frac{\Gamma_t k_{gas} \left(\Phi n_d w (V_m / V_s) \right)^b \exp(m^2 / 2)}{n_d} \right) X^b + 1 \tag{23}$$

n_d is density of donor electron, which is assumed to be constant, w is the depletion layer width. From Eq. (23) (under $D \gg 2w$), it can be seen that the gas sensing mechanism is controlled by the potential barrier of the contact between wires. Furthermore, the potential barriers are independent of the cylinder size and therefore, the sensitivity is independent of the diameter of nanowire, D.

Under $D > 2w$

In this case, the depletion layer has effect on both electron density in the wires and the potential barrier of the contacts between the wires. Thus, the sensor resistance is controlled by surface depletion layer and the potential barrier in this case. The conductance related to the nanowire after oxygen adsorption is given as:

$$G = \frac{e \mu_0 [e] \pi (D - 2w)^2}{4l} \tag{24}$$

where μ_0 is the crystal electron mobility, l is the distance between electrodes. It can be seen that the gas-sensing mechanism depends on both the width and the height of the contact potential barriers (Sysoev et al., 2009, Rothschild&Komem, 2004). Thus, the sensor resistance due to surface depletion layer and potential barrier is represented by

$$R = R_0 \left(\frac{D}{D - 2w} \right)^2 \exp\left(m^2 / 2\right). \tag{25}$$

From Eq. (12), (8) and using $[e]=n_0$, the sensor response formula can be given as (Wongrat et al., 2012)

$$S_g = \left(\frac{\Gamma_t k_{gas} \left(\Phi n_d w (V_m / V_s) \right)^b \exp\left(m^2 / 2\right)}{n_d} \right) \left(\frac{D}{D - 2w} \right)^2 X^b + 1 \tag{26}$$

From this equation, it can be seen that the sensor response depend not only on the potential barrier between wires but also on the size of nanowire.

Under *D≤2w*

In this case, the depletion layer has effect only on the electron density in the wires and can be regarded as fully depleted cylinders. The fully depleted cylinders are occurred when the Fermi level is totally controlled by surface states under nearly flat energy bands and so potential barrier can be neglected. Therefore, the sensor resistance is controlled only by the surface depletion in this case.

3. Experimental, results and discussions

3.1. Sensor fabrication

The MOS nanowires have been synthesized by thermal oxidation technique. This technique has been successfully used for synthesizing ZnO or CuO by simply heating pure Zn and Cu material source, respectively. The process is usually conducted in a cylindrical furnace. For the synthesis of ZnO nanowire as shown in Fig. 5, Zn thin films or thick films were screened or evaporated on alumina substrate. Then, they were sintered at temperature in ranging of 500-700ºC to form the nanostructure. For the synthesis of CuO nanowire, the commercial grade copper plate with thickness of 0.1 mm was cut and cleaned by alcohol in an ultrasonic bath for 2 min and dried at room temperature. The copper plate was loaded into a center of a tube furnace at 600°C at normal atmosphere for oxidation reaction.
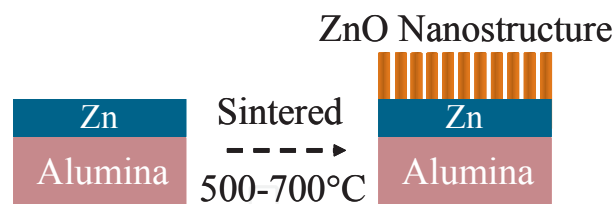

Figure 5. Schematic diagram of the synthesis of ZnO nanowire on alumina substrate by thermal oxidation technique.

The sensors were fabricated by putting gold paste as inter-digital electrodes on the top of the sensors surface and putting a heater underneath the alumina substrate as shown in Fig 6. The heater for the sensor was made from nickel-chromium which could control temperature in the range 280-380 ºC. The operating temperature was measured by a thermocouple placed on the middle of the sensor.

3.2. Setup for ethanol sensing characteristic measurement

A set up for the ethanol sensing characteristic measurement was shown in Fig. 7. The sensing response and recovery characteristics of MOS sensors were studied in a gas flow chamber under a dynamic equilibrium. Electrical measurements were performed using a volt-amperometric
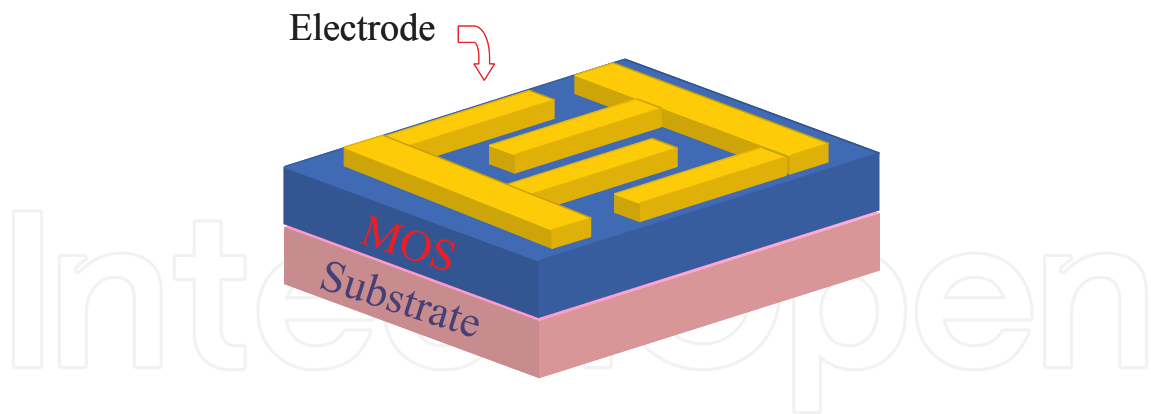
Figure 6. Schematic diagram of the fabricated sensor structures.

technique. A constant bias voltage of 5 V was applied to the sensor. Another voltage was applied to the heater coil used for heating the sensor and maintaining at a desired operating temperature. A thermocouple was employed to monitor the sensor temperature. The ammeter, voltmeter, and thermocouple signals were monitored and recorded via an interfaced personal computer. The ethanol sensing properties of the device were observed by the resistance change under an ethanol vapor atmosphere at different operating temperatures. Since our goal was to apply as an alcohol breath analyzer, the ethanol vapor at various concentrations was generated from ethanol solutions using alcohol simulator (GUTH Laboratories, Inc., Harrisburg, PA). The function of this alcohol simulator was to simulate alcohol concentration at conditions similar to exhaled human breath, being varied for ethanol concentration of 50–1,000 ppm for this experiment. A set up for the ethanol sensing characteristic measurement was illustrated in Fig. 7. The sensor sensitivity is defined by the ratio of the electrical resistance of the sensor in air and the electrical resistance of the sensor in ethanol vapor.
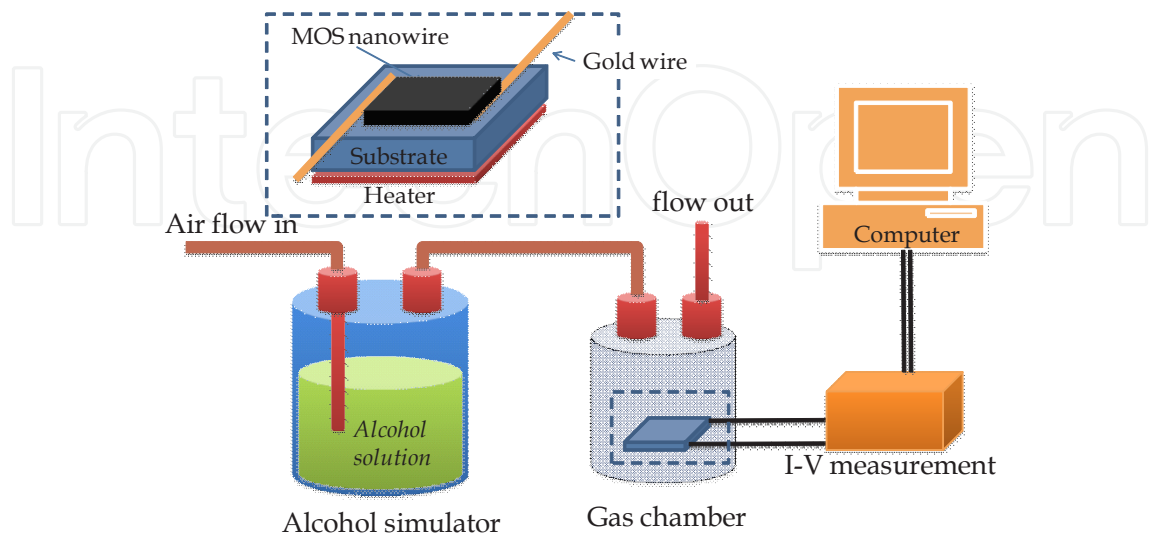

Figure 7. Schematic diagram of a set up for the ethanol sensing characteristic measurement.

3.3. ZnO and CuO nanowires

For the synthesis of ZnO nanowires, it was found that the nanowires exhibit the belt-like or wire-like structures with sharp tip. The diameter and length were in the range of 100-500 nm and 2-7 µm, respectively. For the synthesis of CuO nanowires, the nanowires having a diameter of 100–400 nm and the length of around several micrometers were observed. The different morphologies of ZnO and CuO nanowires were shown in Fig 8. It can be seen that Fig 8 (a) and (b) were for the thick film morphologies. No nanowires were observed in this case representing as the bulk case. Fig 8 (d) and (f) were for vertical aligned and non-vertical aligned ZnO nanowires, respectively. The vertical aligned ZnO nanowires were prepared by zinc screening technique but non-vertical alignment of ZnO nanowires were prepared by zinc evaporation technique. And finally Fig 8 (g) was for the CuO nanowires (Raksa et al., 2005).
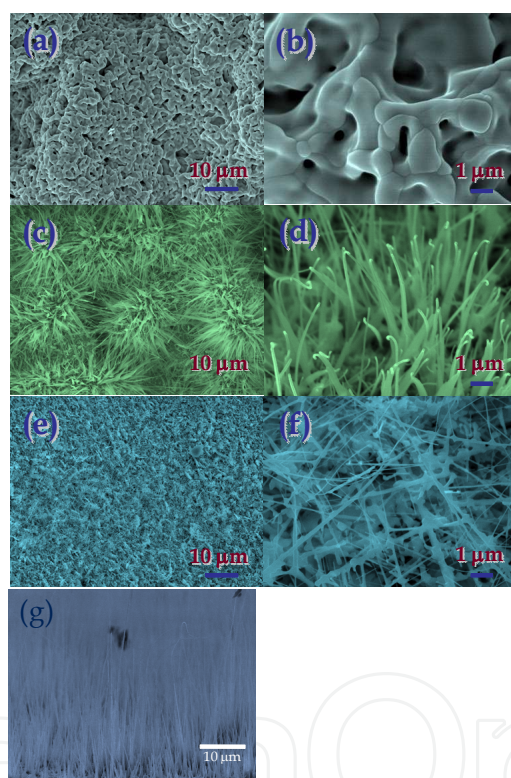

Figure 8. FE-SEM images of bulk ZnO (a, b), ZnO nanowires (c-f), and CuO nanowires (g).

3.4. Response and recovery curve

The resistance response and recovery characteristics of ZnO and CuO gas sensor that exposed to ethanol concentration in range of 50-1,000 ppm at the optimum operating are shown in Fig. 9 (a) and (b), respectively. At the beginning, the measured resistance is steady in air atmosphere and then, the resistance of ZnO sensor drops sharply in ethanol atmosphere and recovers to the initial value after removing ethanol vapor. While the resistance of CuO sensor rapidly rises in ethanol atmosphere and falls back after removing ethanol. The decrease and increase of

resistance under the ethanol atmosphere is due to the n-type and p-type conducting of ZnO and CuO, respectively as discussed earlier.

The sensitivity of ZnO sensors with different sizes and morphologies at different ethanol concentration are summarized in Table 2. The sensitivity of sensor is defined as R_a/R_g (reverse for CuO case) when R_a was the resistance of sensor in air and R_g was the steady resistance of sensor in ethanol. The sensor sensitivity strongly depends on size and morphology of the sensors. This size and morphology dependence will be discussed in a later section.
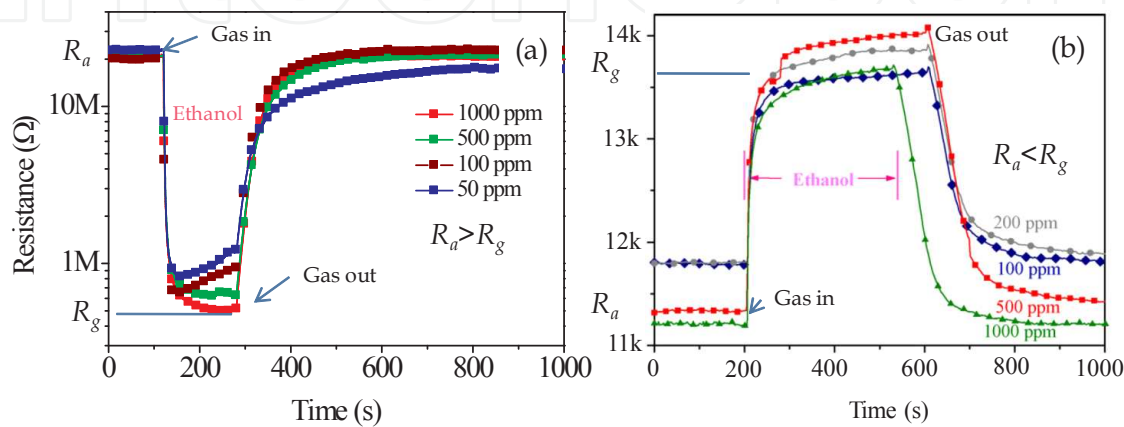

Figure 9. The response and recovery curve of n-type and p-type MOS sensor for ZnO nanowires (a) and CuO nano-wires (Raksa et al., 2005) (b), respectively.

Morphology	*Diameter (nm)*	Sensitivity (50 ppm)	Sensitivity (100 ppm)	Sensitivity (500 ppm)	Sensitivity (1000 ppm)
bulk	-	1.3	1.6	2.0	2.2
Nanowire (screening)	100-500	3.1	3.9	6.4	8.7
Nanowire(evaporation)	11-104	17	24	30	40

Table 2. Sensor sensitivity of sensor with different ZnO sizes and morphologies.

3.5. Linear relation and Sensitivity enhancement based on metal oxide nanowires

Sometimes, a compact form of the sensitivity relation on gas concentration can be rewritten as

$$S_g = aX^b + 1 \tag{27}$$

$$a = \frac{\Gamma_t k_{gas} \left(\dfrac{\sigma_0 \Phi V_m}{V_s} \right)^b}{n_0} \tag{28}$$

where *a* is a controllable parameter and X is a concentration of gas. At the optimum operating temperature condition, the relation between the sensitivity and gas concentration can be rewritten as:

$$\log(S_g - 1) = \log a + b \log X. \tag{29}$$

It can be seen that $\log(S_g-1)$ has a linear relation with $\log X$ having a slope of *b* value. Thus, *b* value which represents oxygen ion species on the surface of MOS sensors can be obtained from a slope of a plot between $\log(S_g-1)$ and $\log X$. The value of the constant b is normally around either 0.5 or 1, depending on the charge state of the surface ion. The adsorbed oxygen ion is O^{2-} for *b* of 0.5, the adsorbed oxygen ion is O^- for *b* of 1.

The plots between $\log(S_g-1)$ and $\log X$ of some works as listed in Table 1 was displayed in Fig 10. It was found that the value *b* of all sensors is close to 0.5 suggesting that the adsorbed surface oxygen species on ZnO sensor is O^{2-}. In addition, this suggests that the oxygen adsorption species on the surface is independent on the size and morphology of ZnO regardless of bulk, microstructure or nanostructure.
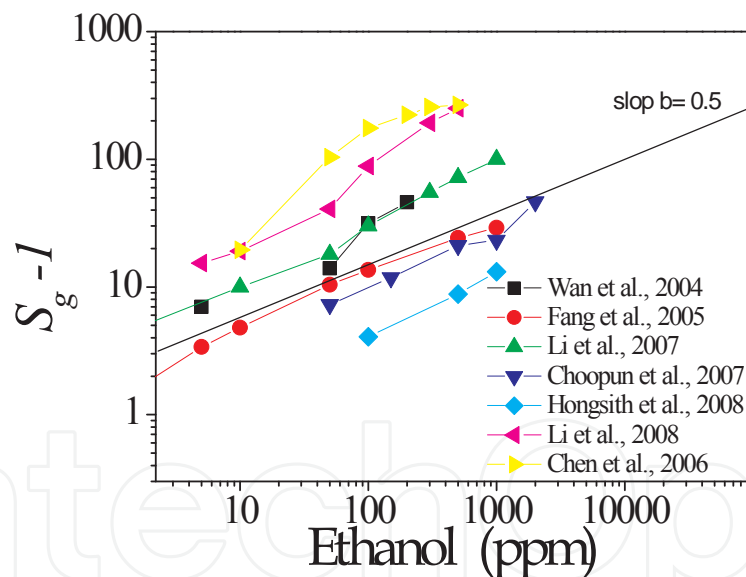

Figure 10. Plot of sensor response (*Sg-1*) and ethanol concentration in log scale for ethanol sensor based on different ZnO morphologies. The linear line in the graph has a slope of 0.5.

3.6. Sensor sensitivity

In the section 2 we have explained the sensing formula for n-type and p-type MOS sensor. In this section, we will explain the sensing parameters for understanding in the mechanism of resistance change under air atmosphere and gas atmosphere and will discuss in term of the size and morphology dependence on the sensor sensitivity.
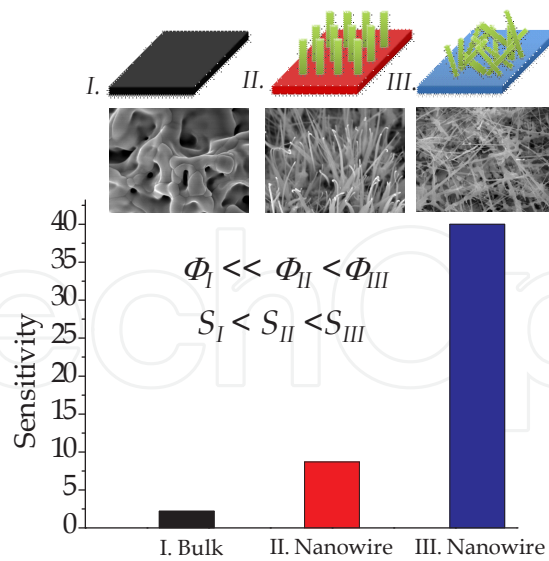
Figure 11. Sensor sensitivity for different ZnO sizes and morphologies with ethanol concentration of 1,000 ppm.

Let consider a sensitivity of MOS gas sensor based on the different sizes and morphologies as seen in Fig. 11, it can be divided into three cases of MOS ethanol gas sensor.

3.6.1. Bulk ZnO

From Table 2, the sensitivity of a bulk ZnO sensor shows the lowest value compare with that of nanostructures. It can be simply explained by using Eq. (8). The sensing parameter of the surface-to-volume ratio is low for the bulk sensor and thus, the oxygen ion surface density is low resulting in low sensitivity.

3.6.2. Large size nanowires

From Table 2, it can be seen that the sensitivity of MOS sensor based on vertical aligned nanowires (zinc screening nanowires) is higher than that of bulk. The sensitivity is 8.7 for vertical aligned nanowires sensor at 1,000 ppm of ethanol compared to that of about 2 for bulk ZnO gas sensor. The higher sensitivity of MOS sensor based on vertical aligned nanowires can be explained in terms of surface-to-volume ratio parameter (Φ) by using Eq. (11) or (15). Since Φ is proportional to sensitivity, the larger Φ due to nanostructure gives the higher sensitivity for the case of vertical aligned nanowires even though the nanowires are not aligned along the conducting direction.

3.6.3. Small size nanowires

It can be seen in Table 2 that the sensitivity of MOS sensor based on non-vertical aligned nanowires (zinc evaporation nanowires) is even higher than that of zinc screening nanowires (the sensitivity increases from 8.7 to 40). This is due to the combination effects of the surface-to-volume ratio and the depletion layer and can be explained by using Eq. (15). The non-vertical aligned nanowires exhibit smaller diameter (11-104 nm) indicating higher surface-to-volume

ratio. Also, the diameter of nanowires is comparable to the depletion layer width (two times of Debye length; about 10 nm for ZnO) indicating strong effect of the depletion layer. Thus, the surface-to-volume ratio parameters (Φ) increases and the difference between diameter and the depletion layer width (D-$2L_d$) decreases resulting in the increase of the sensor sensitivity as indicated in Eq. (15).

3.7. Ultra high gas sensing by adding novel metal

In addition, the sensor sensitivity can be further enhanced up to several folds by using adding novel metal technique.There have been several reports on sensitivity enhancement due to metal doping or metal adding effect. We have also reported on the sensitivity enhancement due to gold nanoparticles (AuNPs) on the surface of ZnO (Wongrat et al., 2012).As shown in Fig 12, the sensitivity of ZnO:AuNPs exhibits maximum value of 478 at ethanol concentration of 1,000 ppm while the sensitivity of pure ZnO nanostructure sensor is about 40.
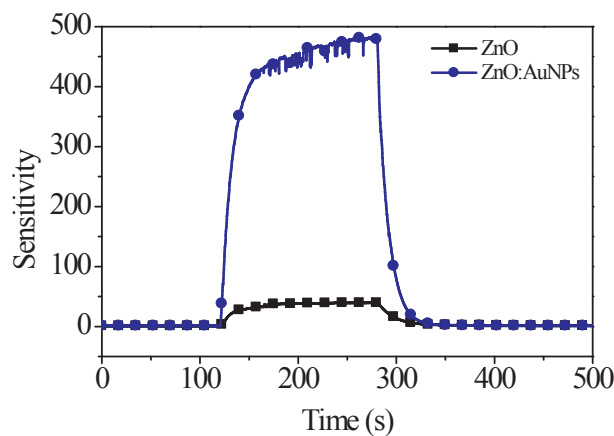

Figure 12. Ultra high sensitivity of ZnO sensor withAuNPs on the surface at ethanol concentration of 1,000 ppm (Wongrat et al., 2012).

The metal adding effect can be simply explained in our model by using Eq. (15), (17) and (26). It can be seen that the sensitivity is proportional to the reaction rate constant, k_{gas} and k_{Oxy}, through the oxygen density. Basically, the reaction rate constant can be affected by noble metals (such as Au, Pd, Pt etc.) in MOS sensors due to the catalytic effect. Thus, metal adding causes an increasing of reaction rate constant and resulting in enhancement of the sensor sensitivity.

The evidence for having higher k_{gas} can be observed from the sensor resistance in the ethanol ambient. The sensor resistance under ethanol ambient of ZnO:AuNPs sensor is about 200 kΩ which is less than of pure ZnO nanostructure sensor(500 kΩ) suggesting higher k_{gas}. In addition, the evidence for having higher k_{Oxy}, can be observed from the sensor resistance in air. The highest resistance in air of ZnO:AuNPs sensor is about 100 MΩ which is more than of resistance of pure ZnO nanostructure sensor (20 MΩ).The increase of resistance in air suggests that the gold metal catalytically activates the dissociation of molecular oxygen due to higher reaction rate that results in increasing an amount of the oxygen adsorption molecules. Therefore, electrons in ZnO nanowire are captured by oxygen adsorption to form oxygen ion

and hence ZnO nanowire loses more electrons and causes the larger depletion layer at ZnO surface resulting in higher resistance.

Therefore, the sensitivity enhancement of ZnO sensors with noble metal is due to catalytic effect in both ethanol adsorption reaction k_{gas} and oxygen adsorption reaction k_{Oxy} through the oxygen density. In the other words, the ultra-high sensitivity of ZnO sensors with noble metal can be explained by an increase of both parameters of k_{gas} and w (depletion layer width) as described in Eq. (26).

4. Summary

The MOS nanostructures, especially nanowires have been demonstrated to be an excellent candidate as a gas sensing device. The gas sensors based on MOS nanowires are promising due to feasibility for ultrahigh sensitive sensors or ppb-level sensors. The simple and low-cost technique of thermal oxidation technique is effectively used to prepare the MOSs nanowires. The sensing characteristics of the MOS sensors strongly depend on sizes and morphologies of ZnO nanostructures. The sensitivity formulas have been developed in order to explain all circumstances of gas sensors based on MOS nanowires. The size and morphology dependences on the sensitivity have been explained in terms of the two important parameters including surface-to-volume ratio and depletion layer width. The experimental sensing characteristics of ZnO sensors are in good accordance to the developed formulas. This suggests that the sensing formulas are a powerful tool in sensor design and also can be applied for sensors based on other MOSs such as SnO_2, TiO_2, MoO_3 or WO_3, etc. In addition, the sensor sensitivity can be further enhanced up to several folds by using adding novel metal technique and can be simply used the developed sensitivity formula for explanation in term of the depletion layer parameter.

Symbols used

k Reaction rate

X Density, Concentration, of X

n, n_0 Electron carrier density

Γ Time constant

R_a Resistance in air

R_g Resistance in active gas

S_g Sensitivity

Φ Surface to volume ratio

σ, σ_0 Oxygen ion surface density

V_m Volume of material

V_s Volume of system

C_g Ethanol concentration

L_d Debye length

ε Static dielectric constant

q Electrical charge of carrier

k_B Boltzmann constant

T Temperature (K)

Acknowledgements

Author details

Supab Choopun[1,3], Niyom Hongsith[2,3] and Ekasiddh Wongrat[2]

1 Department of Physics and Materials Science, Faculty of Science, Chiang Mai University Chiang Mai, Thailand

2 School of Science, University of Phayao, Phayao, Thailand

3 ThEP Center, CHE, Bangkok, Thailand

References

[1] Rothschild, A, Komem, Y, & Appl, J. Phys., (2004).

[2] Li, C. C, Du, Z. F, Li, L. M, Yu, H. C, Wan, Q, & Wang, T. H. Appl. Phys.Lett., (2007).

[3] Li, C. C, Du, Z. F, Yu, H. C, & Wang, T. H. Thin Solid Films, (2009).

[4] Comini, E, Faglia, G, & Sberveglieri, G. Zhengwei Pan and Zhong L. Wang, Appl. Phys.Lett., (2002).

[5] Comini, E, Faglia, G, & Sberveglieri, G. Electrical-Based Gas Sensing." in Solid State Gas Sensing, E. Comini, G. Faglia, and G. Sberveglieri (Ed), Springer Science+Business Media, LLC, New York, (2009). , 47.

[6] Wongrat, E, Pimpang, P, & Choopun, S. Appl. Surr. Sci., (2009).

[7] Wongrat, E, Hongsith, N, Wongratanaphisan, D, Gardchareon, A, & Choopun, S. Sens. Actuators B, (2012).

[8] Neri, G, Bonavita, A, Micali, G, Donato, N, Deorsola, F. A, Mossino, P, Amato, I, & Benedetti, B. D. Sensor. Actuator B, (2006).

[9] Zhang, H. N, Li, Z. Y, Liu, L, Xu, X. R, Wang, Z. J, Wang, W, Zheng, W, Dong, B, & Wang, C. Sensor. Actuator B, (2010).

[10] Son, J. Y, Lim, S. J, Cho, J. H, & Seong, W. K. and Hyungjun Kim,Appl. Phys.Lett., (2008).

[11] Xu, J. Q, Zhang, Y, Chen, Y. P, Xiang, Q, Pan, Q. Y, & Shi, L. Y. Mater. Sci. Eng. B, (2008).

[12] Arshak, K, & Gaidan, I. Mater. Sci. Eng. B, (2005).

[13] Bie, L. J, Yan, X. N, Yin, J, Duan, Y. Q, & Yuan, Z. h. Sens. Actuators B, (2007).

[14] Hongsith, N, Viriyaworasakul, C, Mangkorntong, P, Mangkorntong, N, & Choopun, S. (2008).

[15] Hongsith, N, Wongrat, E, Kerdcharoen, T, & Choopun, S. Sens. Actuators B, (2010).

[16] Wang, N, Cai, Y, & Zhang, R. Q. Mater. Sci. Eng. R-Rep., (2008).

[17] Yamazoe, N, & Shimanoe, K. Sens. Actuators B, (2008).

[18] Feng, P, Wan, Q, & Wang, T. H. Appl. Phys.Lett., (2005).

[19] Raksa, P, Gardchareon, A, Chairuangsri, T, Mangkorntong, P, Mangkorntong, N, & Choopun, S. Ceramics International, (2009).

[20] Wan, Q, Li, Q. H, Chen, Y. J, & Wang, T. H. Appl. Phys.Lett., (2004).

[21] Choopun, S, Hongsith, N, Mangkorntong, P, Mangkorntong, N, & Physica, E. (2007).

[22] Sysoev, V. V, Schneider, T, Goschnick, J, Kiselev, I, Habicht, W, Hahn, H, Strelcov, E, & Kolmakov, A. Sens. Actuators B, (2009).

[23] Lee, Y. C. Hui Huang, O.K. Tan, and M.S. Tse, Sens. Actuators B, (2008).

[24] Chen, Y. J, Zhu, C. L, & Xiao, G. Sens. Actuators B, (2008).

[25] Chen, Y. J, Zhu, C. L, & Xiao, G. Nanotechnology, (2006).

[26] Liu, Y. X, Gao, C. T, Pan, X. J, An, X. Y, Xie, Y. Z, Zhou, M, Song, J, & Zhang, H. L. Z.Y.

[27] Liu, Q, Zhao, Y. H, & Zhang, E. Q. Xie, Appl. Surr. Sci., (2010).

[28] Song, X. F, Wang, Z. J, Liu, Y. B, Wang, C, & Li, L. J. Nanotechnology, (2009).

[29] Yang, Z, Li, L. M, Wan, Q, Liu, Q. H, & Wang, T. H. Sens. Actuators B, (2008).